The role of upper hybrid waves in magnetic reconnection

W. M. Farrell, M. D. Desch, K. W. Ogilvie, and M. L. Kaiser
NASA/Goddard Space Flight Center, Greenbelt, Maryland, USA

K. Goetz
School of Physics and Astronomy, University of Minnesota, Minnesota, USA

Received 17 April 2003; revised 3 October 2003; accepted 4 November 2003; published 20 December 2003.

[1] Wind observations of upper hybrid (UH) waves adjacent to a magnetic X-line are compared with simultaneous Wind electron observations to clarify wave-electron interactions. Electron beams and ''football'' ($T_{\|} > T_{\perp}$) distributions accompany the UH waves. The energy density of the inward-directed beams, at 10^{-14} J/m^3, is sufficient to supply the free energy for the waves. The electron beams may be part of the larger Hall current system, and the UH wave/electron instability represent a Hall current dissipation process (i.e., an effective resistance) which removes energy as the currents travels along the separatrix. *INDEX TERMS:* 2712 Magnetospheric Physics: Electric fields (2411); 2740 Magnetospheric Physics: Magnetospheric configuration and dynamics; 2744 Magnetospheric Physics: Magnetotail; 2748 Magnetospheric Physics: Magnetotail boundary layers; 2772 Magnetospheric Physics: Plasma waves and instabilities. **Citation:** Farrell, W. M., M. D. Desch, K. W. Ogilvie, M. L. Kaiser, and K. Goetz, The role of upper hybrid waves in magnetic reconnection, *Geophys. Res. Lett.*, *30*(24), 2259, doi:10.1029/2003GL017549, 2003.

1. Introduction

[2] On 1 April 1999, the Wind spacecraft made two fortuitous close encounters with distant (~60 Re) magnetotail X-line regions, passing well into the region where ions become unmagnetized [*Oieroset et al.*, 2000, 2001, 2002; *Farrell et al.*, 2002]. The first Wind near-encounter of the day occurred near 08:00 UT as the X-line passed inward towards Earth. Analysis of this event has revealed the following: a clear signature of quadrupole magnetic fields associated with Hall currents consistent with collisionless magnetic reconnection [*Oieroset et al.*, 2001], passage from fast Earthward to fast tailward flows [*Oieroset et al.*, 2000], the presence of low energy (~300 eV) electron beams flowing near the separatrix [*Oieroset et al.*, 2001], and the discovery of energetic (~300 keV) electron flux increases near the center of the region [*Oieroset et al.*, 2002]. Low frequency whistler-mode wave activity was ubiquitous, appearing at approximately the same intensities both within and outside the region [*Oieroset et al*., 2002], suggesting that the additional wave generation via a lower hybrid drift instability (LHDI) was not occurring in the region. Unfortunately, the Wind Waves FFT processor [*Bougeret et al.*, 1995] was sampling with 20 minute intervals until 0900 UT and associated VLF plasma wave activity could not be measured during the event. The observation of a well-developed Hall current system is consistent with recent Geotail [*Nagai et al.*, 2001] and Polar [*Mozer et al.*, 2002; *Scudder et al.*, 2002] observations.

[3] The second event for that day occurred near 10:22 UT, as the (an) X-line region moved outward towards the tail [*Oieroset et al.*, 2000]. This event revealed the clear passage from fast tailward, to low density slow lobe plasma, to fast earthward flows in the course of about 20 minutes [*Oieroset et al.*, 2000], copious signatures of electron holes (electrostatic solitary waves also appearing as broadband electrostatic noise) in the fast earthward and tailward flows, and very intense (~40 mV/m) upper hybrid bursts detected near the separatrix (lobe/plasma sheet boundary) [*Farrell et al.*, 2002]. ULF whistler mode waves were relatively weak (~0.1 mV/m) and ubiquitous both within and outside the region, again suggesting that the LHDI was not a dominant process in the region [*Farrell et al.*, 2002].

[4] In this work, we focus on the second Wind X-line passage at 10:22 UT when both the Waves FFT receiver and Wind SWE solar wind electron [*Ogilvie et al.*, 1995] measurements are available. Our primary objective is to determine the nature of the UH wave/electron interaction by examination of the electron distributions and wave activity in and around the separatrix. We particularly want to understand the flow of energy in the wave/electron interaction: Are electrons generating wave activity via instability/spontaneous emission process? Or conversely, are the waves (independently generated by some other process) strong enough to make anomalous electron movement and diffusion? As we demonstrate, the answer is determined by the degree to which the electrons are in resonance with the waves.

2. Observations

[5] The Wind Waves and 3DP [*Lin et al.*, 1995] measurements used in this presentation have been described previously [*Farrell et al.*, 2002]. The additional data in this work is derived from Wind's solar wind experiment (SWE), and its two detection systems, the vector electron and ion spectrometer VEIS and Strahl electron detection system [*Ogilvie et al.*, 1995]. The VEIS detection system monitors electron flux at energies between 7 and 2480 eV, and is capable of creating 576-point electron distributions every 6 seconds in magnetic field coordinates, with measurements to within about 5° of the ambient magnetic field. The Strahl detector is specifically designed to examine electron flux in a $60^\circ \times 40^\circ$ window about the ambient magnetic field. The system was originally designed to measure narrowly-beamed electron flows originating from the solar corona

0094-8276/03/2003GL017549

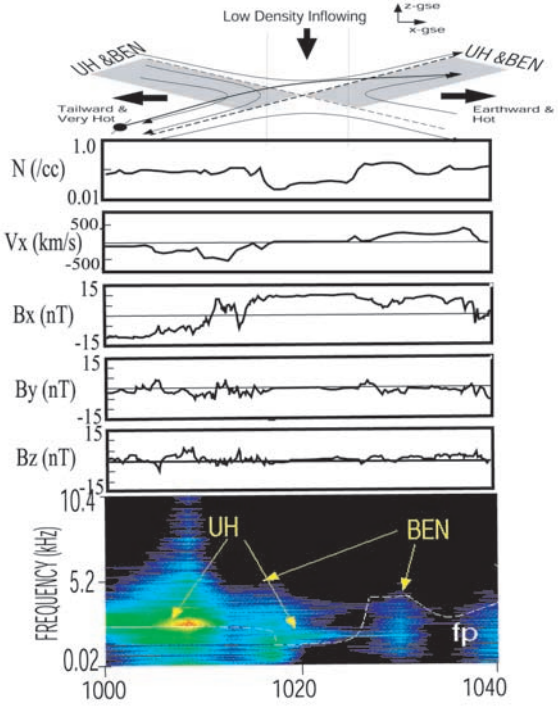

Figure 1. An illustration of the Wind/X-line geometry (separatrix is dashed line), the Wind 3DP and MFI magnetoplasma density, speed, and B-field (from *Oieroset et al.* [2000]), and Wind Waves spectrogram from 20–10400 Hz, showing the UH emission near 1008 UT.

(the Strahl electrons [*Fairfield and Scudder*, 1985]). The instrument yields a detailed ~3° resolution map of electron flux about the magnetic field line at a given energy, and cycles through 58 eV to 1160 eV every seven minutes.

[6] Figure 1 shows the geometry of the spacecraft through the 40 minute passage, five line plots of the associated 3DP and MFI [*Lepping et al.*, 1995] measurements (from *Oieroset et al.* [2000]) and a Waves FFT spectrogram of electric field activity between 20 Hz and 10400 Hz. As evident in the figure, Wind was in the tailward fast flow ($V_x < 0$) until 1017 UT. At that time, it crossed the separatix and remained in the low density, low speed inflowing lobe plasma for about 9 minutes. Near 1026 UT, the spaceraft again crossed the separatrix and moved into the earthward-directed fast plasma flows ($V_x > 0$). Figure 1 shows that B_y develops a relatively large (-5γ) negative excursion from about 1005–1020 UT in the tailward flowing region, and a small ($+2-3\gamma$) positive upswing near 1026 UT in the earthward flow, possibly indicating a magnetic field produced by Hall currents.

[7] As indicated in the Waves spectrogram in Figure 1, wave activity was very substantial in the hot tailward flowing plasma downstream of the lobe/plasma sheet boundary. Both upper hybrid bursts and broadband electrostatic noise (the FFT signature of nonlinear electrostatic solitary waves [*Kojima et al.*, 1997]) were detected in the fast outflowing plasma from the region. A particularly intense UH burst was observed at 1008 UT in the tailward fast flowing plasma. The corresponding SWE electron distribution at this time (Figure 2) shows the presence of an X-line directed electron beam of ~600 eV (at $V_b \sim -1500$ km/sec), superimposed on top of a thermalized flattop distribution with $T_{\|} > T_{\perp}$. This flattop distribution extends from the edge of the primary core at 50 eV to 600 eV.

[8] Similar flattop distributions were also observed by Geotail in the vicinity of the X-line separatrix and have been referred to as 'football' shaped distributions [*Hoshino et al.*, 2001a]. PIC simulations of the X-line region indicate that such football distributions are found very near the lobe/plasma sheet boundary [*Hoshino et al.*, 2001a] and are believed to be initially isolated bump-on-tail distributions of a few hundred eV that evolve into plateau or "flat-tops" via wave/electron interaction. As demonstrated in their high-resolution PIC code [*Hoshino et al.*, 2001a], the flattops closest to the separatrix also contain the inward-directed Hall current electron beam (similar to our observation in Figure 2) and these beams/football distributions were shown to be associated with intense magnetized Langmuir waves (i.e., UH emissions). Both the simulation and actual Wind observations suggest that UH waves are the most intense mode in the region [*Farrell et al.*, 2002]. In the case shown in Figures 1 and 2, Wind SWE made the fortuitous

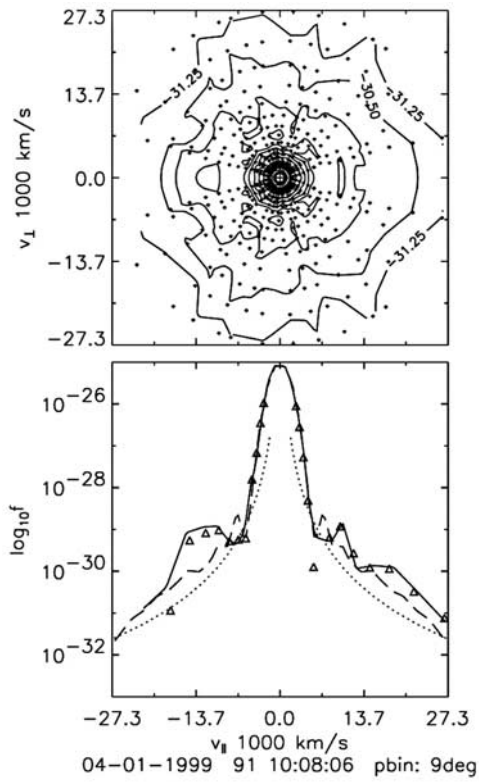

Figure 2. A Wind SWE electron distribution concurrent with the UH wave observation. Note the presence of an inward-directed electron beam (moving toward the X-line) near -1.4×10^7 m/sec (~600 eV) along with a flat-top "football" like distribution ($T_{\|} > T_{\perp}$). In the bottom panel the reduced distributions are displayed with the solid line representing an extrapolated $f_{\|}$, the triangles representing the nearest real $f_{\|}$ measurement, the dashed line representing the extrapolated $f_{\perp}$ and dotted line representing the zero-count level.

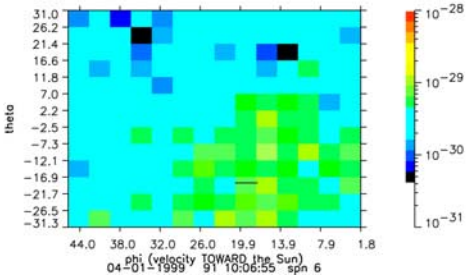

Figure 3. The SWE Strahl electron angular distribution at 541 eV along the (−) B direction is shown. The sensor is viewing tailward. The angular extent of a clear X-line (inward) directed beam at 541 eV is shown. Note that the overall beam width is about 20°, and there are multiple peaks about B.

measurement of the actual bump-on-tail beam electrons prior to full wave relaxation or thermalization into football distributions, the electron observations made nearly simultaneous with Waves detection of an intense UH bursts.

[9] Figure 3 shows the anti-sunward Strahl 541 eV detector at 10:06:55 UT (closest measurements to the UH activity). A clear presence of a quasi-field aligned electron beam moving earthward toward the X-line region is shown. This beam is comparable to that in the left hand side of Figure 2 (also moving along -B towards the X-line). Note that the beam, when analyzed with 2–4° resolution, has multiple peaks oriented at various angles (∼15°) relative to B.

[10] Of critical importance is the determination of the electron beam origin. Simulations [*Hoshino et al.*, 2001a, 2001b] suggest that the cold beam moving inward toward the X-line (directly analogous to our beam in Figures 2 and 3) consists of accelerated lobe electrons and is associated with the Hall current system (current outward, electron beam inward). Note in Figures 1 and 2 that the occurrence of the electron beam and the UH emissions is near the same period of time B_y is strongly negative near 1009 UT, consistent with this electron beam/Hall current association. As described by *Hoshino et al.* [2001a] the wave/electron instability then thermalize the beams to form plateau/football distributions. If we assume the beam comes from a region of parallel electric field extending the ion skin depth (∼700 km [*Oieroset et al.*, 2001]), the DC electric field would be on the order of ∼1 mV/m, like that suggested in *Pritchett* [2001].

3. UH Wave Growth and Implications for Resonant and Non-Resonant Electrons

[11] The electron beam energy density ($\sim n_b m_e v_b^2$) is on the order of 10^{-14} J/m^3 (for a beam density 10^{-3} that of ambient and beam velocity near 10^7 m/s). Conversely, the energy density of the waves ($\varepsilon_o E^2$) is on the order of 10^{-15} J/m^3. Hence, it appears the electrons are of larger power and could be the free energy source for the waves. However, the wave powers are a large fraction of the beam energy, larger than the typical few percent conversion in an electrostatic beam-related stimulated emission process [*Klimas and Farrell*, 1994]. We surmise that the electron beams, observed with 6 second resolution during this period, are partially relaxed. They would be of greater density and velocity if the temporal resolution of the electron measurement (unrealistically) matched the wave growth (i.e., if the electron distribution was observed prior to wave energy transfer).

[12] In order to understand the energy flow from electrons to waves, we performed a stability analysis. The quasi-electrostatic dispersion relation [*Lin et al.*, 1984; *Hudson and Roth*, 1984] for a three component plasma is considered: a cold high density component, a weak hot Maxwellian electron component representing the thermal football distributions, and an bi-Maxwellian electron beam component, with $f \propto \exp -(v - V_b)^2/u_b^2$, V_b being the beam speed. The dispersion relation is

$$1 + D_c + D_f + D_b = 0 \tag{1}$$

where subscript c is for cold, f is for football, and b is for beam, $D_c = -\cos^2\theta\ \omega_{pc}^2/\omega^2 - \sin^2\theta\ \omega_{pc}^2/(\omega^2 - \omega_g^2)$, $D_f = A_f\,[1 + z_f\,B_f \sum_{N=-\infty}^{\infty} Z(z_f - c_f(n))]$, $D_b = A_b\,[1 + z_b\,B_b \sum_{N=-\infty}^{\infty} Z(z_b - c_b(n))]$, $A_{f,b} = 2\omega_{pf,b}^2/k^2u_{f,b}^2$, $B_{f,b} \sim (2\pi k_\perp^2 \rho_{f,b}^2)^{-1/2}$, $z_f = \omega/k_\parallel u_f$, $z_b = (\omega - k_\parallel V_b)/k_\parallel u_b$, $c_{f,b} = n\omega_g/k_\parallel u_{f,b}$, and Z is the plasma dispersion function. The component specific variables ω_p, u, and ρ are the electron plasma frequency, electron thermal speed, and electron gyroradius, respectively, and ω_g is the electron gyrofrequency. The wave mode $\omega = \omega(k)$ is derivable by setting the real part of equation (1) to zero and assuming $z_{f,b} < 1$:

$$D_{real} \sim 1 - \cos^2\theta\,\omega_{pc}^2/\omega^2 - \sin^2\theta\,\omega_{pc}^2/\left(\omega^2 - \omega_g^2\right) + A_f + A_b = 0. \tag{2}$$

The growth rate is $\gamma = -(dD_{real}/d\omega)^{-1}\,\mathrm{Im}(D_f + D_b)$ and is

$$\gamma \sim -\pi^{1/2}(dD_{real}/d\omega)^{-1}\left[A_f\,z_f\,B_f \sum_{n=-1}^{n=1} \exp\left(-(z_f - c_f)^2\right) + A_b\,z_b\,B_b \sum_{n=-1}^{n=1} \exp\left(-(z_b - c_b)^2\right)\right] \tag{3}$$

where $dD_{real}/d\omega \sim 2\cos^2\theta\ \omega_{pc}^2/\omega^3 + 2\sin^2\theta\ \omega_{pc}^2\,\omega/(\omega^2 - \omega_g^2)^2$. Note that the analysis is performed only for the Landau, normal cyclotron and anomalous cyclotron resonance (n = 0, ± 1). The first term in equation (3) and $dD_{real}/d\omega$ are both positive for all ω, keeping $\gamma < 1$. Positive wave growth ($\gamma > 1$, instability) occurs when $z_b < 1$ (i.e., $\omega/k_\parallel < V_b$). This condition is consistent with wave/electron resonance in regions where the slope of the distribution is positive. The football distribution provides a consistent negative contribution that acts to damp wave growth. Figure 4 shows the oblique ($\theta = 40°$) UH wave growth from a beam with $n_b = 10^{-3}\,n_c$, $V_b = 1.7 \times 10^7$ m/s, and $u_b = 0.5 \times 10^7$ m/s and football distribution with $n_f = 10^{-4}\,n_c$ and $u_f = 2 \times 10^7$ m/s, similar to the case shown in Figure 2. The analysis shows a clear region near $k = 0.001–0.002$ m^{-1} where the wave growth is positive ($\gamma_{max} \sim 0.001\ \omega_p$). Note that $\omega/k_\parallel$ is $\sim 1.4 \times 10^7$ m/sec at maximum growth, consistent with being on the positive side of the beam

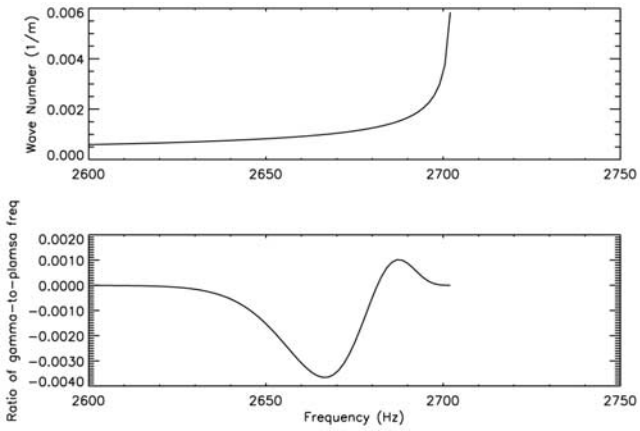

Figure 4. Wave mode and growth rate for the UH emission driven by an electron beam and a warm, football-like distribution (see text for detailed values).

distribution. We conclude the electron beams can indeed drive the UH wave activity. The maximum growth rate varies directly with beam density (e.g., for $n_b = 5 \times 10^{-3}\ n_c$, $\gamma/\omega_p \sim 0.005$). Reducing football densities act to increase the bandwidth of unstable wave modes.

[13] The role and importance of this beam energy dissipation process depends upon the importance of the beams themselves. If the beams are associated with Hall currents, beam energy loss via wave/electron instabilities acts as a natural resistance for the electron portion of the Hall current. In essence, the Hall currents are reduced (reduction in overall velocity in $j_- = neV_b$) or even disrupted via the instability, disallowing complete current closure around the X-line. In essence, the instability is nature's way of attempting to impede the motion of the inward-moving electrons relative to the unmagnetized ions.

[14] We note in Figure 2 that a weaker electron beam is present along the +B direction, flowing away from the X-line. This beam may be associated with a local return currents driven by a polarization electric field associated with the separation of the primary inward-moving electrons and unmagnetized ions. This local return current flows in an attempt to keep ion-electron balance.

[15] The UH waves can have a major impact on non-resonant electrons as well. These non-resonant electrons are defined as those with phase speeds well away from the UH wave phase speed so as not to be trapped by the UH wave potential. Recently, *Drake et al.* [2003] suggested, via simulation, that electron holes (electrostatic solitary waves) can be effective scattering sites (creating perpendicular momentum) for electrons near the X-line region. Wind observations near the X-line indicated the presence of such electron holes, but with substantially smaller amplitudes (40 times less) than the UH waves [*Farrell et al.*, 2002]. In contrast, stochastic interactions between UH waves and low energy non-resonant electrons can lead to impulsive and large accelerations in the electron's parallel and perpendicular momentum, particularly in large UH wave fields [*Akimoto and Karimabadi*, 1988]. The UH wave perturbation strength is $\varepsilon \sim \omega_c E \sin\alpha/\omega c B_o$, with E the wave amplitude, B_o the ambient magnetic field and α the wave propagation angle relative to B_o (*Akimoto and Karimabadi* [1988], equation 15). This wave perturbation is largest (with greatest electron energization and scattering) when the ambient magnetic field gets small, like in the central X-line region. Such stochastic wave-electron trajectories may have been simulated [*Hoshino et al.*, 2001b, Figure 5]. A similar stochastic diffusion process was recently invoked to explain the fast energization of radiation belt electrons via VLF electromagnetic waves [*Summers and Ma*, 2000].

4. Conclusions

[16] We conclude that (1) energetic electron beams flow along the separatrix, along with a thermal "football" shaped plateau distribution. (2) UH waves occur in coincidence with the beams, and are the agents that act to thermalize the beams into the plateau football-shaped form. (3) The energy density of the observed beam at 10^{-14} J/m^3 is about a factor of 10 larger than the wave energy density values, suggesting the beam drives the waves. (4) The UH wave growth can occur in regions of the electron distribution where $df/dv_{||} > 0$, like those shown in Figures 2 and 3. The wave growth is at the expense of beam energy. Consequently, the UH waves are a Hall current dissipation mechanism. Finally, (5) the intense UH waves have a secondary effect on non-resonant electrons, stochastically accelerating a portion of the population to high energies possibly explaining the relativistic flux increases reported by *Oieroset et al.* [2002].

References

Akimoto, K., and H. Karimabadi, Relativistic structure of stochastic wave-particle interactions, *Phys. Fluids*, *31*, 1505, 1988.

Bougeret, J.-L., et al., Waves: The radio and plasma wave investigation on the Wind spacecraft, *Space Sci. Rev.*, *71*, 231, 1995.

Drake, J. F., et al., Formation of electron holes and particle energization during magnetic reconnection, *Science*, *299*, 873, 2003.

Fairfield, D. H., and J. D. Scudder, Polar Rain: Solar corona electrons in the earth's magnetosphere, *J. Geophys. Res.*, *90*, 4055, 1985.

Farrell, W. M., M. D. Desch, M. L. Kaiser, and K. Goetz, The dominance of electron plasma waves near a reconnection X-line, *Geophys. Res. Lett.*, *29*(19), 1902, doi:10.1029/2002GL014662, 2002.

Hoshino, M., K. Hiraide, and T. Mukai, Strong electron heating and non-Maxwellian behavior in magnetic reconnection, *Earth Planets Space*, *53*, 627, 2001a.

Hoshino, M., T. Mukai, T. Terasawa, and I. Shinohara, Suprathermal electron acceleration in magnetic reconnection, *J. Geophys. Res.*, *106*, 25,979, 2001b.

Hudson, M. K., and I. Roth, Thermal fluctuations from an artificial ion beam injection into the ionosphere, *J. Geophys. Res.*, *89*, 9812, 1984.

Klimas, A. J., and W. M. Farrell, A splitting algorithm for Vlasov simulation with filamentation filtration, *Comp. Phys.*, *110*, 150, 1994.

Kojima, H., et al., Geotail waveform observations of broadband/narrowband electrostatic noise in the distant tail, *J. Geophys. Res.*, *102*, 14,439, 1997.

Lepping, R. P., et al., The Wind magnetic field investigation, *Space Sci. Rev.*, *71*, 207, 1995.

Lin, C. S., et al., Correlation of auroral hiss and upward electron beams near the polar cusp, *J. Geophys. Res.*, *89*, 925, 1984.

Lin, R. P., et al., A three-dimensional plasma and energetic particle investigation for the Wind spacecraft, *Space Sci. Rev.*, *71*, 125, 1995.

Mozer, F. S., S. D. Bale, and T. D. Phan, Evidence of diffusion regions at the subsolar magnetopause crossing, *Phys. Rev. Lett.*, *89*, 15,002, 2002.

Nagai, T., et al., Geotail observations of the Hall current system: Evidence of magnetic reconnection in the magnetotail, *J. Geophys. Res.*, *106*, 25,929, 2001.

Ogilvie, K. W., et al., A comprehensive plasma instrument for the Wind spacecraft, *Space Sci. Rev.*, *71*, 55, 1995.

Oieroset, M., et al., Walen and varience analysis of high-speed flows observed by Wind in the midtail plasma sheet: Evidence for reconnection, *J. Geophys. Res.*, *105*, 25,247, 2000.

Oieroset, M., et al., In situ detection of collisionless reconnection in the Earth's magnetotail, *Nature*, *414*, 2001.

Oieroset, M., et al., Evidence for electron acceleration up to ~300 keV in the magnetic reconnection diffusion region of earth's magnetotail, *Phys. Rev. Lett.*, *89*, 195,001, 2002.

Pritchett, P. L., Collisionless magnetic reconnection in a three dimensional open system, *J. Geophys. Res.*, *106*, 25,961, 2001.

Scudder, J. D., et al., Fingerprints of collisionless reconnection at the separator, I, Ambipolar Hall signatures, *J. Geophys. Res.*, *107*, doi:10.1029/2001JA000126, 2002.

Summers, D., and C. Ma, A model for generating relativistic electrons in the earth's inner magnetosphere based on gyroresonant wave-particle interactions, *J. Geophys. Res.*, *105*, 2625, 2000.

W. M. Farrell, M. D. Desch, K. W. Ogilivie, and M. L. Kaiser, NASA/Goddard Space Flight Center, Code 695, Greenbelt, MD 20771, USA. (william.farrell@gsfc.nasa.gov)

K. Goetz, School of Physics and Astronomy, University of Minnesota, Minneapolis, MN 55455, USA.